Supplementary Information

The ghost of nestedness in ecological networks

Phillip P.A. Staniczenko[1,*], Jason C. Kopp[1,†] & Stefano Allesina[1,2,‡]

[1]Dept. Ecology & Evolution, University of Chicago, Chicago, IL, USA
[2]Computation Institute, University of Chicago, Chicago, IL, USA
[*]pstaniczenko@uchicago.edu, Corresponding Author
[†]jasonckopp@gmail.com
[‡]sallesina@uchicago.edu

6th December, 2012

[*]**Corresponding Author:** Phillip Staniczenko, Department of Ecology and Evolution, University of Chicago. 1101 E. 57th, Chicago, IL, 60637, USA. Email: pstaniczenko@uchicago.edu

Contents

1 Supplementary Figures and Table

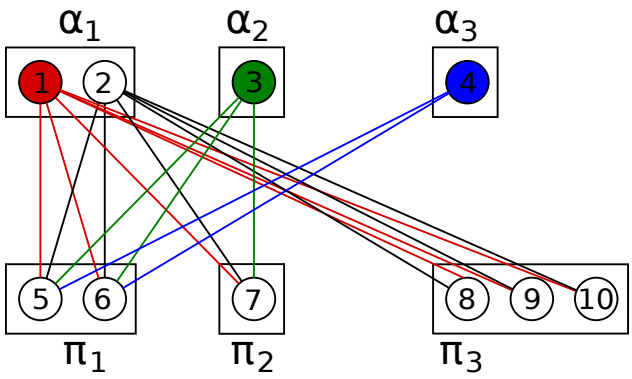

Supplementary Figure S1: **Double Nested Graph (DNG) notation and construction.** For the $DNG(2,1,1;2,1,3)$, there are 4 animals (top) and 6 plants (bottom). The animals are partitioned into three boxes of size 2, 1, and 1 (the α's), the animals in three boxes of size 2, 1, and 3 (the π's). The nodes in box α_i connect to all the nodes in boxes $\pi_1, \ldots, \pi_{k+1-i}$. This is shown for one node in α_1 (red), α_2 (green) and α_3 (blue).

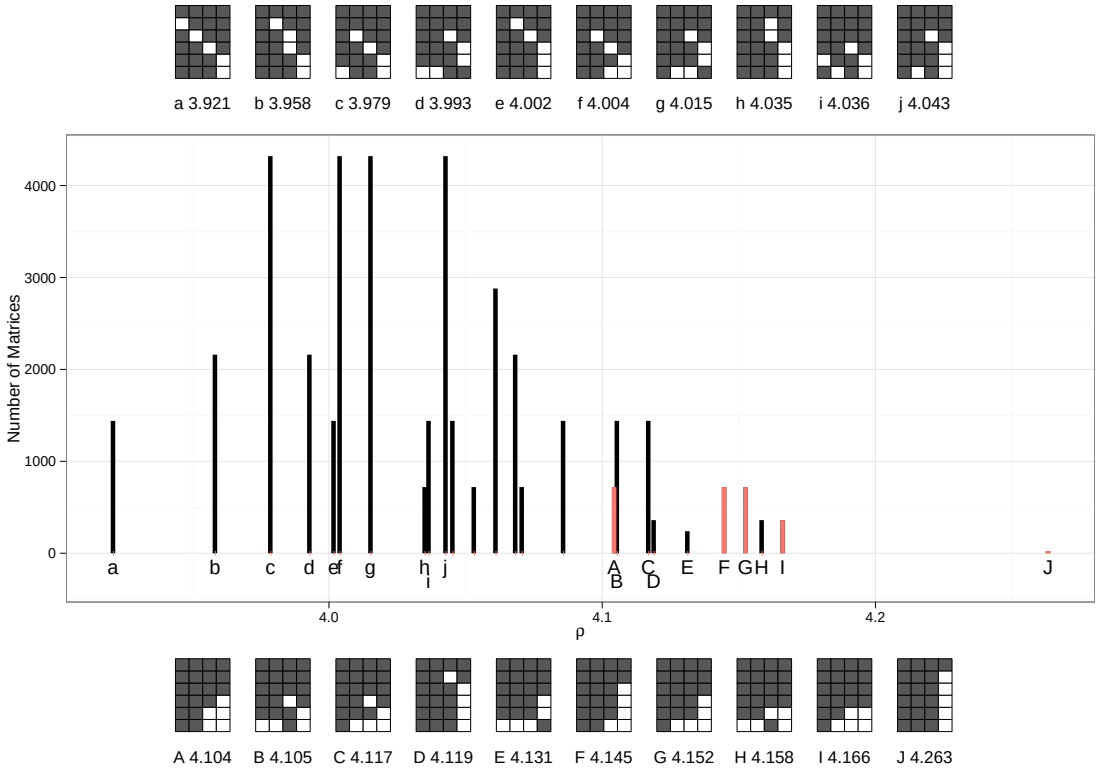

Supplementary Figure S2: **Binary nestedness and eigenvalues, second example.** Spectral radius (largest eigenvalue) distribution for all connected binary graphs with $|P| = 6$, $|A| = 4$ and $|E| = 19$. Adding two edges greatly reduces the total number of possible configurations compared to the $|E| = 17$ case (Figure 1, main text). There are 42,504 possible matrices with this parameter combination, of these, 42,384 are connected (shown in figure). Among the connected graphs, 2,544 are perfectly nested (coloured orange), and have higher spectral radii than most other matrices (all perfectly nested matrices are contained in the top 15.06% of the distribution). As in Figure 1 of the main text, the maximum spectral radius is associated with a perfectly nested matrix: $DNG(3, 1; 1, 5)$, matrix J. Matrices with the lowest spectral radii display interaction patterns that depart most severely from perfect nestedness (top series).

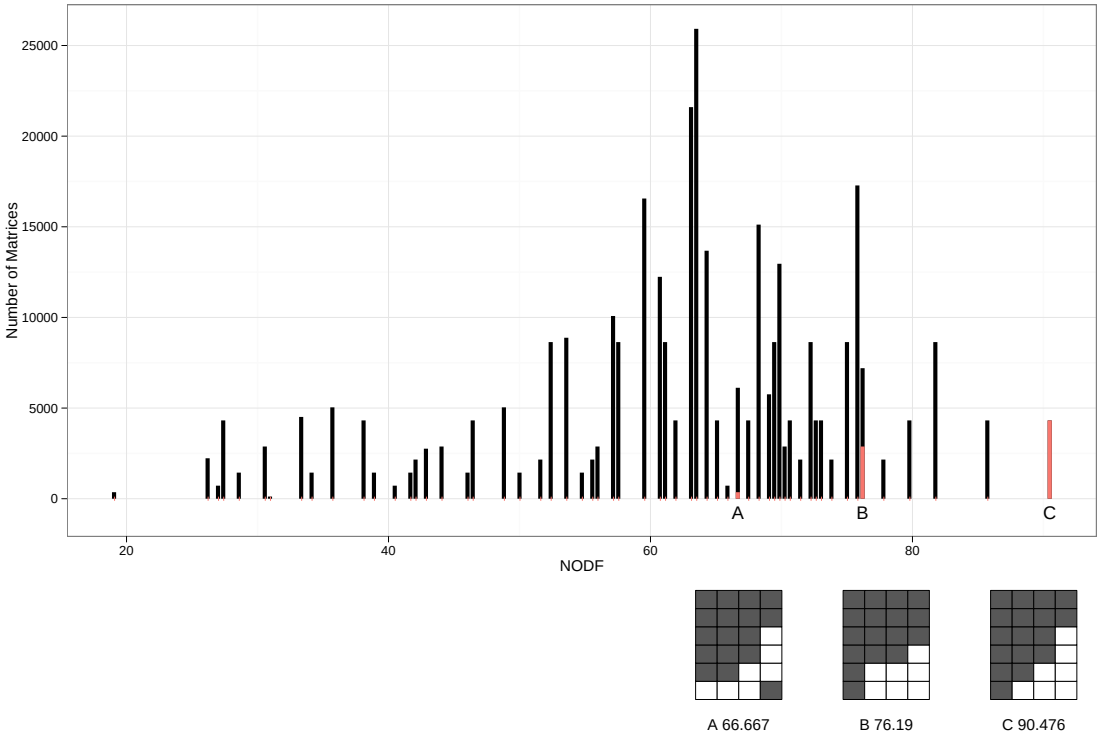

Supplementary Figure S3: **Binary nestedness and NODF.** Distribution of NODF values for all connected binary graphs with $|P| = 6$, $|A| = 4$ and $|E| = 17$. There are 346,104 possible incidence matrices with this parameter combination, and of these, 339,192 are connected (shown in figure). Among the connected graphs, 7,560 are perfectly nested (coloured orange) (all perfectly nested matrices are contained in the top 40.46% of the distribution compared to 4.59% when using the spectral radius). Note that unlike the spectral radius (Figure 1 in the main text), many perfectly nested matrices as well as not perfectly nested matrices share the same value of NODF, e.g., matrix A, which is not perfectly nested, has the same NODF value as perfectly nested matrices.

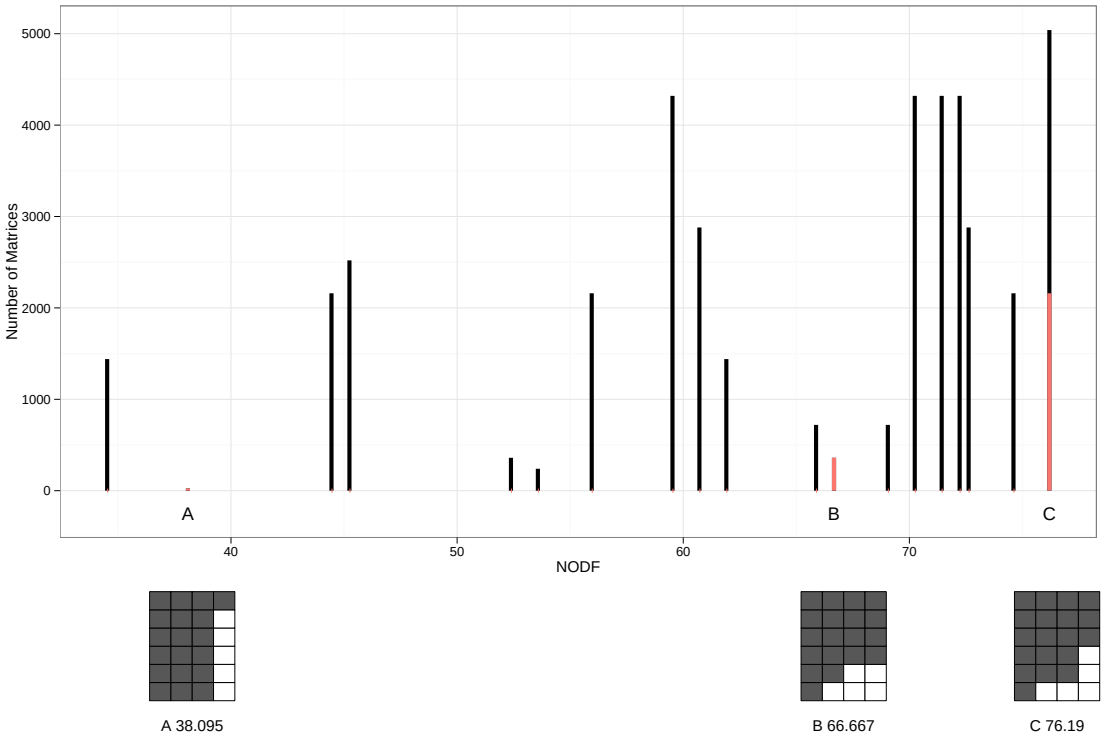

Supplementary Figure S4: **Binary nestedness and NODF, second example.** Distribution of NODF values for all connected binary graphs with $|P| = 6$, $|A| = 4$ and $|E| = 19$. There are 42,504 possible matrices with this parameter combination, of these, 42,384 are connected (shown in figure). Among the connected graphs, 2,544 are perfectly nested (coloured orange) (all perfectly nested matrices are contained in the top 96.60% of the distribution compared to 15.06% when using the spectral radius, Supplementary Figure S2). As in the case with $|E| = 17$ (Supplementary Figure S3), many perfectly nested matrices as well as not perfectly nested matrices share the same value of NODF.

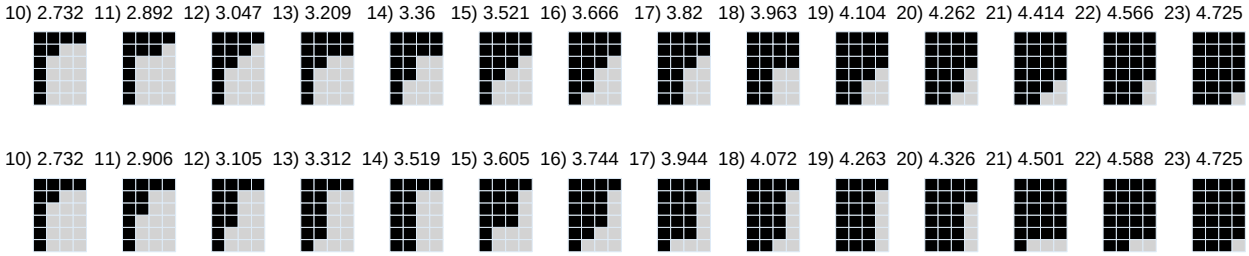

Supplementary Figure S5: **Minimum and maximum spectral radius for perfect nestedness.** Nested perfectly binary structures with the minimum (top series) and maximum (bottom series) spectral radius for $|P| = 6$, $|A| = 4$ and $|E| = \{10, 11, \ldots, 23\}$. Notice that the matrix yielding the minimum eigenvalue for a given number of connections $|E|$ can be obtained by adding one edge to the arrangement found for $|E| - 1$ connections, while this is not the case for the matrices yielding the maximum eigenvalue (e.g., going from 14 to 15 connections in the bottom series).

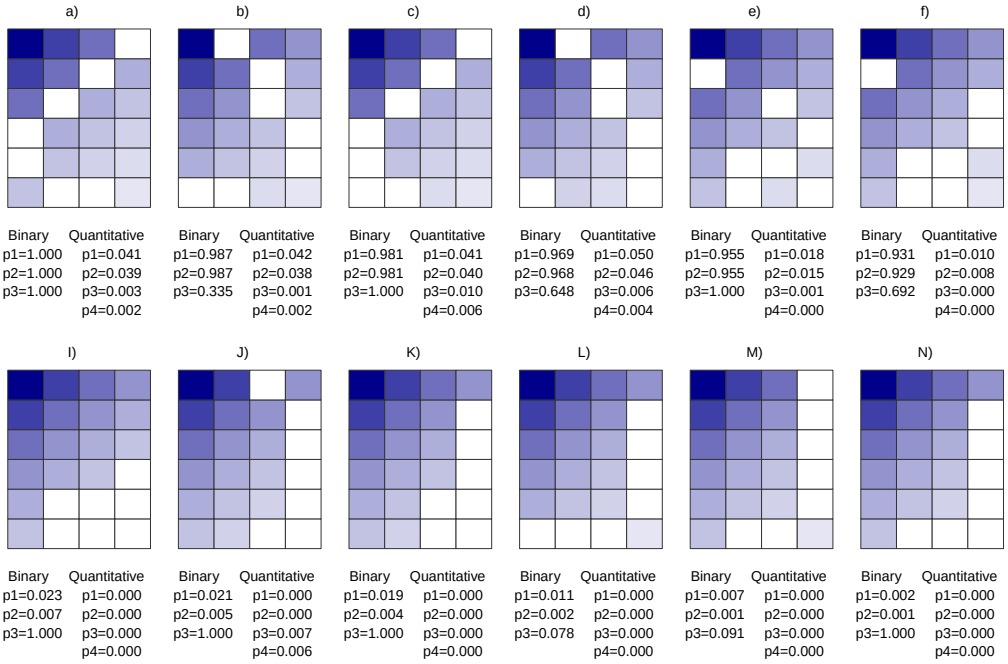

Supplementary Figure S6: **Quantitative nestedness and binary structure.** A perfectly nested quantitative pattern is overlaid onto a set of perfectly nested, close to perfectly nested and non-nested binary matrices from Figure 1 of the main text. Darker colours indicate larger coefficient values, and white squares represent zero entries; results for the seven binary and quantitative tests (p-values, lower values indicate greater nestedness) are given below each matrix. For the perfectly nested and close to perfectly nested binary structures (bottom series), the tests for quantitative nestedness are always highly significant. Remarkably, matrices that are significantly non-nested in their binary form (top series) become highly nested when the nested quantitative pattern is taken into account. This suggests that the quantitative structure of a network is likely to dominate any underlying binary pattern.

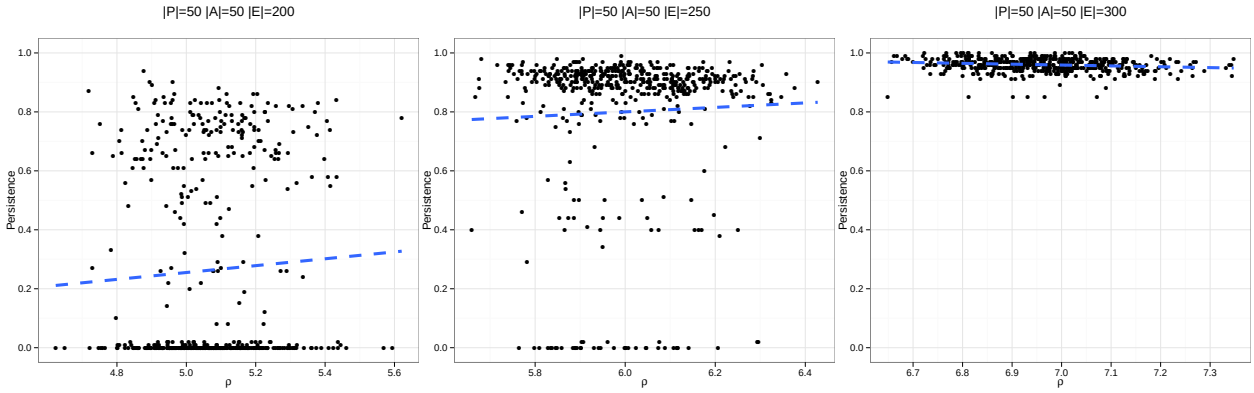

Supplementary Figure S7: **Effect of nestedness and connectance on species persistence.** We simulated the obligate mutualism system in Equation S3 for $|P| = 50$ plants and $|A| = 50$ animals, and with a variable number of edges $|E|$ (and hence connectance) between the two sets of species. In all cases, the parameters and initial conditions were taken from the original article by Thébault & Fontaine [9]. We integrated the system numerically from $t = 0$ to $t = 100,000$ and recorded the fraction of surviving species (persistence, y-axis). The dashed lines are best-fit linear regressions. The number of edges from left to right are 200, 250 and 300. For $|E| = 200$ most of the networks are disconnected, while in the other two cases most of the networks are connected. We observe no significant effect of nestedness (spectral radius of the community matrix with zero on the diagonal, ρ, x-axis) on persistence, except for the most-connected case $|E| = 300$ where the slope is negative (-0.03, $p < 3.78 \cdot 10^{-5}$). In no case do we observe a significant positive contribution of ρ to persistence, as was claimed in [9].

Supplementary Table S1: **Nestedness of ecological networks.** 10,000 randomisations per test per web.

Web	Type	Rows	Cols	Edges	Bp1	Bp2	Bp3	Qp1	Qp2	Qp3	Qp4	Ref
1	para	14	20	57	<0.001	<0.001	0.209	0.698	0.693	0.812	0.803	[34]
2	para	19	9	51	<0.001	<0.001	0.242	0.156	0.155	0.335	0.331	[35]
3	mut	65	27	374	<0.001	<0.001	0.146	<0.001	<0.001	0.070	0.112	[36]
4	para	7	29	78	<0.001	<0.001	<0.001	0.100	0.083	0.615	0.800	[37]
5	para	10	40	91	<0.001	<0.001	<0.001	0.160	0.146	0.322	0.405	[38]
6	para	31	144	384	<0.001	<0.001	0.082	<0.001	<0.001	0.297	0.458	[39]
7	para	14	51	114	<0.001	<0.001	<0.001	0.062	0.056	0.478	0.648	[40]
8	para	17	53	158	<0.001	<0.001	0.002	0.033	0.032	0.390	0.501	[40]
9	para	33	97	316	<0.001	<0.001	0.005	0.122	0.120	0.452	0.475	[41]
10	para	5	23	51	0.011	<0.001	0.002	0.653	0.593	0.760	0.843	[42]
11	ant	41	51	285	<0.001	<0.001	0.548	<0.001	<0.001	<0.001	<0.001	[43]
12	ant	19	10	38	0.883	0.606	0.847	0.379	0.280	0.298	0.283	[44]
13	pol	13	13	71	<0.001	<0.001	0.693	0.002	0.002	0.892	0.886	[45]
14	pol	100	58	534	<0.001	<0.001	0.335	<0.001	<0.001	0.008	0.007	[46]
15	pol	103	54	467	<0.001	<0.001	0.202	0.097	0.096	0.704	0.698	[46]
16	pol	114	32	309	<0.001	<0.001	0.819	0.003	0.005	0.142	0.136	[47]
17	pol	88	40	278	<0.001	<0.001	0.534	0.671	0.665	0.889	0.894	[48]
18	pol	79	25	299	<0.001	<0.001	0.560	<0.001	<0.001	<0.001	<0.001	[49]
19	pol	8	14	33	0.004	<0.001	0.403	0.028	0.012	0.362	0.376	[50]
20	pol	44	13	143	<0.001	<0.001	0.035	0.146	0.137	0.386	0.393	[51]
21	pol	13	14	52	<0.001	<0.001	0.920	0.007	0.005	0.785	0.650	[52]
22	pol	12	10	30	0.151	0.031	0.591	0.263	0.197	0.424	0.430	[52]
23	pol	56	9	103	<0.001	0.005	0.046	0.052	0.040	0.319	0.318	[53]
24	pol	32	7	59	<0.001	<0.001	0.467	0.003	0.002	0.481	0.472	[54]
25	pol	34	13	141	<0.001	<0.001	<0.001	0.639	0.634	0.978	0.985	[55]
26	pol	23	8	35	<0.001	<0.001	0.681	0.009	<0.001	0.596	0.581	[56]
27	pol	27	8	47	0.022	<0.001	0.895	0.334	0.239	0.727	0.676	[56]
28	fw	125	120	2290	<0.001	<0.001	<0.001	<0.001	<0.001	<0.001	0.573	[57]
29	seed	9	31	119	<0.001	<0.001	0.484	0.056	0.054	0.739	0.723	[58]
30	seed	11	13	53	<0.001	<0.001	0.464	0.002	0.002	0.577	0.570	[59]
31	seed	71	19	283	<0.001	<0.001	<0.001	0.108	0.102	0.683	0.738	[60]
32	seed	57	14	136	<0.001	<0.001	<0.001	<0.001	<0.001	0.067	0.401	[60]
33	seed	71	15	288	<0.001	<0.001	0.008	0.265	0.266	0.567	0.572	[60]
34	seed	32	7	59	0.038	<0.001	0.048	0.158	0.024	0.475	0.631	[60]
35	seed	33	10	70	<0.001	<0.001	0.051	<0.001	<0.001	0.071	0.214	[60]
36	seed	14	65	249	<0.001	<0.001	0.434	0.004	0.003	0.568	0.581	[61]
37	seed	19	29	211	<0.001	<0.001	0.611	0.896	0.896	0.956	0.955	[62]
38	seed	14	11	46	0.008	0.002	0.588	0.810	0.795	0.955	0.957	[63]
39	fruit	21	7	50	<0.001	<0.001	0.875	0.241	0.193	0.724	0.679	[64]
40	fruit	16	24	67	<0.001	<0.001	0.785	<0.001	<0.001	0.677	0.621	[65]
41	fruit	19	33	94	<0.001	<0.001	0.723	0.023	0.020	0.388	0.384	[65]
42	fruit	12	22	46	<0.001	<0.001	0.860	0.015	0.002	0.722	0.572	[65]
43	fruit	14	20	50	<0.001	<0.001	0.875	0.014	0.007	0.511	0.401	[65]
44	pol	61	17	146	<0.001	<0.001	0.621	0.077	0.074	0.332	0.335	[66]
45	pol	35	15	84	<0.001	<0.001	0.553	0.003	0.004	0.221	0.215	[66]
46	fruit	10	16	110	<0.001	<0.001	0.548	0.922	0.922	0.997	0.997	[67]
47	fruit	18	7	38	0.012	<0.001	0.964	0.163	0.085	0.762	0.653	[68]
48	fruit	29	35	146	<0.001	<0.001	0.064	<0.001	<0.001	0.140	0.241	[68]
49	fruit	17	16	121	<0.001	<0.001	0.663	0.312	0.311	0.598	0.601	[69]
50	fruit	33	25	150	<0.001	<0.001	0.985	0.033	0.031	0.175	0.162	[70]
51	pol	41	97	321	<0.001	<0.001	0.092	0.002	<0.001	0.143	0.155	[71]
52	fruit	8	15	38	<0.001	<0.001	0.490	<0.001	<0.001	0.547	0.544	[72]

2 Supplementary Methods Overview

We begin by introducing the mathematical notation for Double Nested Graphs (DNGs). DNG notation simplifies the representation of perfectly nested binary bipartite networks and also provides insights into their structure. We then relate the structure of bipartite graphs to properties of their matrix representations. Specifically, we show that large dominant eigenvalues correspond to highly nested structures. We provide a way of calculating the number of nested classes, and describe nested patterns for minimal and maximal spectral radius (dominant eigenvalue). By overlaying perfectly-nested quantitative structures onto perfectly nested, close to perfectly nested and non-nested binary networks, we show that the quantitative structure of a network typically dominates any underlying binary pattern.

We then present tests for (not necessarily perfect) binary and quantitative nestedness, as well as a derivation of the condition for finding connected random bipartite graphs. We provide test results for 52 large bipartite ecological networks, and a fuller description of the rescaling procedure used to obtain quantitative species preference matrices. We conclude with a discussion of multispecies models and how they can inadvertently build-in dynamical stability.

3 Double Nested Graph notation

In graph theory, perfectly nested binary bipartite graphs are called Double Nested Graphs (DNGs). Andelić *et al.* [13] introduce a compact notation for DNGs that yields insights into their structure. Each graph (with $|P|$ plants, $|A|$ animals and $|E|$ edges following the convention of the main text) can be described as $DNG(\alpha_1, \alpha_2, \ldots, \alpha_k; \pi_1, \pi_2, \ldots, \pi_k)$ such that: i) $\alpha_i \geq 1$, $\pi_i \geq 1$; and ii) $\sum \alpha_i = |A|$, $\sum \pi_i = |P|$. Using this notation, α_1 can be pictured as a "box" containing the animals with the (same) maximum degree in the network δ_{α_1}, α_2 as another box containing the nodes with the second largest degree δ_{α_2}, and so forth (i.e., $\delta_{\alpha_1} > \delta_{\alpha_2} > \ldots > \delta_{\alpha_k}$). The same holds for the π_i's. For example, consider matrix A in Figure 1 of the main text. This matrix can be

described as $DNG(2,1,1;2,1,3)$: there are two animals with the highest degree ($\delta_{\alpha_1} = 6$), one animal with degree 3, and one with degree 2; two plants share the highest degree ($\delta_{\pi_1} = 4$), one has degree 3 and three have degree 2 (see Supplementary Figure S1). One can construct a binary matrix from the DNG notation in the following way: each node in box α_1 connects to all nodes in boxes π_1, π_2 and π_3; the nodes in α_2 connect to all those in π_1 and π_2; and the nodes in α_3 connect only to those in π_1. In general, the nodes in box α_i connect to all the nodes in boxes $\pi_1, \ldots, \pi_{k+1-i}$.

This notation captures three fundamental aspects of perfectly nested binary graphs. First, in DNGs two nodes with the same degree have the same interaction pattern (in food webs we would call them trophospecies [73]). Second, the number of animal trophospecies is the same as the number of plant trophospecies (k above). This can be explained using the following analogy: a perfectly nested matrix is like a flight of stairs. The stair is composed of steps—changes in degree in the matrix. A well-formed step is composed of the tread (where we step on) and the riser (the vertical part between treads). If we want to build a stair, we need the same number of treads and risers. In the same way, in a perfectly nested matrix we need the same number of discontinuities in the degree distribution of plants and animals. Third, the degree of each species is fully determined by the DNG notation. The degree of a node contained in α_i is simply $\sum_{j=1}^{k+1-i} \pi_j$.

4 The spectral radius of small bipartite graphs

4.1 Eigenvalues and bipartite graphs

The adjacency matrix of a binary bipartite graph with $|S|$ nodes has $|S|$ eigenvalues (not necessarily distinct) such that if λ is an eigenvalue of $\mathcal{A}$ then $-\lambda$ is also an eigenvalue, and the two have the same multiplicity (the number of eigenvectors associated with a given eigenvalue). The spectrum of $\mathcal{A}$ is thus symmetric about the origin. Because $\mathcal{A}$ is a symmetric matrix, all of its eigenvalues are real. The largest eigenvalue of $\mathcal{A}$ is known as its spectral radius $\rho(\mathcal{A})$, and its value is bounded by $\sqrt{|E|}$ from above [13,15]. Moreover, if δ_{min} is the binary degree (i.e., number of connections) of the node with the fewest connections and δ_{max} that of the node with the most connections,

then $\delta_{min} \leq \rho(\mathcal{A}) \leq \delta_{max}$. The eigenvalues are an invariant property of the matrix $\mathcal{A}$. That is, permutation of rows and columns does not affect the eigenvalue distribution. This is important because nestedness is a property of the original graph, and a given graph may be represented by many matrices, so any measure derived from matrix representations—as is typically the case, including here–should not change under permutation of rows and columns.

To test our conjecture that the configuration with largest spectral radius is a perfectly nested binary bipartite graph, we computed the spectral radius for all the possible matrices with $|P|$ plants, $|A|$ animals and $|E|$ edges. This is computationally feasible only for certain parameter combinations as there are $\mathcal{M} = \binom{|P|\cdot|A|}{|E|}$ possible matrices. We performed this analysis for parameter combinations with $\mathcal{M} \leq 10^8$. These are typically moderate sized matrices with low (or high) connectance $C = |E|/(|P| \cdot |A|)$, the fraction of non-zero entries. To generate all the combinations, we used the `gsl_combination` function included as part of the GNU Scientific Library (GSL).

Figure 1 of the main text summarises our findings for the case $|P| = 6$, $|A| = 4$ and $|E| = 17$. There are 346,104 possible matrices. Of these, 339,192 are connected (i.e., any two nodes in the network are joined by a path of edges). Among the connected graphs 7,560 are perfectly nested. Note that the perfectly nested matrices have higher spectral radii than most other matrices. In fact, all of the perfectly nested matrices are contained in the top 4.59% of the distribution. The maximum spectral radius is found for the perfectly nested matrix $DNG(1, 2, 1; 1, 4, 1)$ (matrix N in Figure 1). All matrices with spectral radius greater than that of the nested matrix $DNG(2, 1, 1; 2, 1, 3)$ (matrix A in Figure 1) are either perfectly nested or close to perfectly nested: matrices B, E, F, G, H, J, L and M would become perfectly nested if we were to move just one edge. Matrices with the lowest spectral radii display interaction patterns that depart most severely from perfect nestedness (lowercase letters in Figure 1).

In Supplementary Figure S2 we present the dominant eigenvalue distribution for $|P| = 6$, $|A| = 4$ and $|E| = 19$. Note that adding two edges greatly reduces the total number of possible configurations compared to the $|E| = 17$ case. For these parameters, there are 42,504 possible

matrices. Of these, 42,384 are connected and 2,544 are perfectly nested. All nested matrices are contained in the top 15.06% of the distribution. As before, the maximum spectral radius is associated with a perfectly nested matrix ($DNG(3,1;1,5)$, matrix J).

In all the cases we analysed we found that, among the connected graphs, the largest spectral radius is associated with a DNG. All other perfectly nested graphs have spectral radii close to this maximum value. In the main text, we showed that the positive relationship between the spectral radius and nestedness extends to quantitative matrices (see Figure 2).

As mentioned in the main text, it is worth noting that the (dominant) eigenvector associated with the spectral radius provides a natural way of ordering nodes that best illustrates matrix nestedness.

4.2 Comparison with NODF

NODF [12] is a popular measure of nestedness that is often used in the ecological literature [10,11]. We compared the performance of NODF to the spectral radius by repeating the analysis of the previous section (that resulting in Supplementary Figure S2) but using NODF as a measure of nestedness instead of the spectral radius. The NODF distribution with $|P| = 6$, $|A| = 4$ with $|E| = 17$ is given in Supplementary Figure S3 and is comparable with Figure 1 of the main text, and the distribution with $|E| = 19$ is given in Supplementary Figure S4 and is comparable with Supplementary Figure S2. In both cases, NODF values of perfectly nested matrices span a much larger range than the spectral radius: with $|E| = 17$, all perfectly nested matrices are contained in the top 40.46% of the NODF distribution compared to 4.59% when using the spectral radius; and with $|E| = 19$, all perfectly nested matrices are contained in the top 96.60% of the NODF distribution compared to 15.06% when using the spectral radius. Thus, the statistical ability of NODF to distinguish between patterns of (perfect) nestedness is much lower than the spectral radius.

Unlike the spectral radius, many perfectly nested matrices as well as not perfectly nested ma-

trices share the same value of NODF, an example being the not perfectly nested matrix A in Supplementary Figure S3 sharing the same NODF value as perfectly nested matrices (denoted by the orange colouring in the distribution). Due to these and other well-know limitations of NODF [10,11], we suggest that the spectral radius is a more appropriate measure of nestedness.

4.3 How many classes of perfectly nested matrices?

The 7,560 perfectly nested matrices in Figure 1 of the main text can be classified into one of six classes. That is, each of the 7,560 matrices can be assigned to one of the classes—with each class having a unique DNG representation—by permutation of rows and columns. In Supplementary Figure S2 we observe five such classes. In this section, we show how the number of classes can be computed for arbitrary $|P|$, $|A|$ and $|E|$.

First, we note that the column-wise degree distribution of a perfectly nested matrix is a particular representation of a partition of $|E|$. In number theory and combinatorics, a partition of a positive integer is a way of writing the number, in this case $|E|$, as a sum of positive integers. For example, matrix A in Figure 1 (main text) can be read as a partition of $17 = 6 + 6 + 3 + 2$, while matrix C would be $17 = 6+5+3+3$, and so forth. Thus, the number of classes of nested matrices $\mathcal{N}$ is bounded from above by the partition number $\mathcal{N} \leq N(|E|)$. We can refine this bound and find a recurrence relation that allows us to compute the number of perfectly nested classes exactly.

If we examine the partitions of $|E| = 17$ represented by matrices A, C, D, I, K and N in Figure 1, we note that i) each partition is composed of four terms (number of animals); ii) each term is ≥ 1; iii) each term is $\leq |P|$; and iv) the first term is always $|P|$. Thus, we want to count the number of partitions satisfying these constraints.

Désesquelles [74] provides a recurrence relation for computing the number of partitions of x into y non-zero terms each of which is $\leq z$. The number of partitions with these constraints can be computed as:

$$N(x,y,z) = \begin{cases} N(y(z+1)-x,y,z) & \text{if } x > \frac{y(z+1)}{2} \\ N(x-1,y-1,z)+N(x-y,y,z) & \\ -N(x-y-z,y-1,z) & \text{otherwise} \end{cases} \quad \text{(S1)}$$

The recurrence relation can be solved using the following boundary conditions: i) $N(0,1,z) = 1$; ii) $N(x<0,y,z) = 0$; iii) $N(x \leq z,x,z) = 1$; iv) $N(0<x<y,y,z) = 0$; v) $N(x,x,z) = 1$; and vi) $N(x,1,z) = 1$ if $x \leq z$ and 0 otherwise.

For example, say we want to find the number of partitions of 7 into 3 terms such that each term is ≤ 4. Then we compute $N(7,3,4) = 3$. The partitions are $7 = 4+2+1$, $7 = 3+3+1$ and $7 = 3+2+2$.

Given the above recurrence relation, we can count the total number of classes of perfectly nested matrices for any combination of $|P|, |A|$ and $|E|$. First, we note that each perfectly nested incidence matrix is composed of two parts: the "L" structure (comprising $|P|+|A|-1$ edges that fill the first row and column) and a submatrix, bordered by the "L", that is nested (but not necessarily connected). We can exploit this fact and write down the number of possible (not necessarily connected) perfectly nested submatrices as:

$$\mathcal{N}(|P|,|A|,|E|) = \sum_{i=1}^{|A|-1} N(|E|-(|P|+|A|-1),i,|P|-1) \quad \text{(S2)}$$

where $|A|-1$ is the number of columns in the submatrix, $|P|-1$ is the number of rows and $|E|-(|P|+|A|-1)$ is the number of edges we have to place in the submatrix once we accounted for the "L" structure.

Using this formula we can confirm that the number of perfectly nested structures in Figure 1 should be $\mathcal{N}(6,4,17) = 6$ and those in Supplementary Figure S2, $\mathcal{N}(6,4,19) = 5$. We can compute the exact number of perfectly nested structures for much larger graphs. For example, $\mathcal{N}(30,20,160) = 175,375,723$, $\mathcal{N}(40,40,200) = 1,776,740,177$ and $\mathcal{N}(100,50,300) = 256,215,216$.

4.4 Perfectly nested matrices with minimal and maximal eigenvalue

Given that there may be many classes of perfectly nested binary structures, it is informative to characterise the two classes of perfectly nested matrices yielding the minimum and the maximum spectral radius for a given number of rows, columns and edges.

To produce all possible perfectly nested structures, we modified the algorithm in [75] to generate constrained partitions. In this way, we can directly produce all the unique perfectly nested structures for a given combination of $|P|$, $|A|$ and $|E|$.

In Supplementary Figure S5 we report the perfectly nested structure with the minimum and maximum spectral radius for $|P| = 6$, $|A| = 4$ and $|E| = \{10, 11, \ldots, 23\}$. Notice that the matrix yielding the minimum spectral radius for a given number of connections $|E|$ can be obtained by adding one edge to the arrangement found for $|E| - 1$ connections, while this is not the case for the matrices yielding the maximum spectral radius.

This suggests that we can rapidly build the perfectly nested matrix yielding the minimum possible spectral radius using a greedy algorithm. Starting from the "L" structure described above, the algorithm tries all possible ways to add an edge and chooses the matrix with the minimum spectral radius, additional edges are added using this process until the required number of edges have been placed. In this way, we can compute the minimum possible spectral radius for a perfectly nested matrix with $|P|$ plants, $|A|$ animals and $|E|$ connections.

4.5 Overlaying quantitative nestedness

We can construct a perfectly nested quantitative matrix by taking a perfectly nested binary matrix and filling the coefficients such that they satisfy the definition of perfect nestedness given in the main text. One possible way of overlaying a quantitative pattern is as follows. We begin by forming a distance matrix based on a binary version of the original incidence matrix $\mathcal{B}$. The distance matrix is organised such that non-zero entries in $\mathcal{B}$ take their Manhattan Distance relative to index $(1, 1)$ in $\mathcal{B}$: that is, for $\mathcal{B}_{i,j} > 0$, $\mathcal{D}_{i,j} = \text{Manhattan}((i, j), (1, 1))$, and $\mathcal{D}_{i,j} = 0$ otherwise. The (quantitative

overlay) coefficient value is then given by $\mathcal{B}'_{i,j} = (\frac{3}{4})^{D_{i,j}}$ for $D_{i,j} > 0$, and zero otherwise, with $\mathcal{B}'_{1,1} = 1$. Thus, the further away an element in $\mathcal{B}'$ is from the maximal value at $\mathcal{B}'_{1,1}$, the smaller its coefficient value—in accordance with a perfectly nested quantitative structure. Of course, values other than, but in the region of $\frac{3}{4}$ could be used, giving qualitatively similar results.

The quantitative overlay procedure can be applied to binary configurations other than perfect nestedness by ignoring intermediate zero entries. In Supplementary Figure S6 we overlay a nested quantitative pattern onto a set of perfectly nested, close to perfectly nested and non-nested binary matrices from Figure 1 of the main text. For the perfectly nested and close to perfectly nested binary structures, the tests for quantitative nestedness are always highly significant (tests i to iv, see below). Thus, matrices that are significantly non-nested in their binary form can become significantly nested when a sufficiently strong nested quantitative pattern is overlaid (for example with parameter values in the region of $\frac{3}{4}$). This suggests that the quantitative structure of a network can dominate its underlying binary pattern.

5 Tests for binary and quantitative nestedness

5.1 Binary networks

We showed that perfectly nested binary matrices are associated with large spectral radius. Already, we have a strong test for binary nestedness: compute the spectral radius of an empirical matrix, and, if it is greater than the minimum dominant eigenvalue of a corresponding perfectly nested matrix, then the empirical matrix is almost guaranteed to be nested. However, in general, empirical data are incompatible with perfect nestedness (in many ecological networks, no super-generalists interacting with all of the species in the other class are observed). Here we describe three statistical measures for nestedness that are more applicable to real-world data sets.

In all cases, we take an empirical matrix and compute its spectral radius $\rho(\mathcal{A})$. This is a very well studied problem, and it is quite straightforward to compute the spectral radius of even a very large matrix using, for example, the so-called power method [76]. This method allows fast

computation of the dominant eigenvalue for graphs as large as the World Wide Web [77]. We also build the perfectly nested matrix with the same number of rows, columns and edges that yields the minimum spectral radius ($\mathcal{A}_n$, with spectral radius $\rho(\mathcal{A}_n)$). (Note, if matrix $\mathcal{A}$ is perfectly nested, then $\rho(\mathcal{A}) \geq \rho(\mathcal{A}_n)$.) Finally, we compute the probability p that a randomly constructed matrix $\mathcal{A}'$, which preserves some of the properties of $\mathcal{A}$, is associated with a spectral radius $\rho(\mathcal{A}') \geq \rho(\mathcal{A})$. This allows us to determine the significance of any characterisation of nestedness.

We compute the p-value for both $\mathcal{A}$ and $\mathcal{A}_n$, which can guide us in determining an adequate significance criterion for nestedness. We wish to choose a significance criterion such that any perfectly nested matrix would be assigned a significant p-value. To do so, it is sufficient to choose a significance level equal to the p-value associated with $\mathcal{A}_n$, i.e., if $p < p_{\mathcal{A}_n}$ then the matrix is considered significantly nested. In this way the probability of declaring a perfectly nested matrix not significantly nested is small and tends to zero for large samples. For all but the smallest of networks, $p < 0.05$ is a suitable general significance level for nestedness.

As previously done for other measures of nestedness [10,11], we define three null models to construct the incidence matrix $\mathcal{B}'$ of the symmetric matrix $\mathcal{A}'$: i) preserve $|P|$, $|A|$ and place $|E|$ edges at random within the matrix; ii) as in i), but accept only connected matrices; and iii) as in ii), but conserve the degree distribution (the row and column sums of $\mathcal{B}$). Since measures of nestedness can be very sensitive to matrix size, fill, and configuration [10,11], we used null model implementations that preserve $|P|$, $|A|$ and $|E|$ (null models i and ii) and degree distribution (iii) exactly, and not just their expected values. These three null models are easily extended to quantitative matrices, considered below, wherein we introduce a fourth null model that is specific to weighted graphs.

The three tests are increasingly conservative. Test i) accepts disconnected graphs (as have many other null models in the past [10,11]). We argue that this is not a good choice since perfectly nested graphs cannot be disconnected (by definition, at least one animal interacts with all plants and at least one plant interacts with all animals). Test ii), which accepts only connected matrices,

reflects the approach we took for Figure 1 and Supplementary Figure S2.

Test iii), which is popular in the literature [10,11], poses a problem. We showed above that in perfectly nested binary matrices the degree distribution of animals and plants have the same number of discontinuities. This means that whenever the number of discontinuities in the degree distribution of the animals does not match that of the plants, no perfectly nested matrix with the same degree distribution exists. And so it is not generally possible to compute $\rho(\mathcal{A}_n)$ for null model iii), while this is straightforward for the other null models.

Furthermore, by construction, the set of comparison matrices of test i) includes all those in test ii), which includes all those in test iii). In some cases, the set of comparison matrices for binary test iii) can be small. In fact, since a perfectly nested binary matrix (DNG) is completely defined by its degree distribution, there is only one matrix with the self-same degree distribution. Yet paradoxically, test iii) would classify such a matrix as being (maximally) non-nested. Indeed, the statistical power of test iii) decreases as matrices tend towards perfect nestedness. This is because there are fewer unique (non-isomorphic or non-degenerate) matrices of given $|P|$, $|A|$ and $|E|$ when the degree distribution is highly skewed [78]. This suggests that the application of test iii) to empirical networks, despite its popularity, should be handled with care.

5.2 Condition for finding connected graphs

A classical result for Erdös-Rényi random graphs is the percolation point of connected graphs. For n nodes with probability of connection $C = |E|/(|P| \cdot |A|)$, graphs in which $C > \log(n)/n$ are almost surely connected, while those in which $C < \log(n)/n$ are almost surely disconnected (for the limit $n \to \infty$).

Because for nestedness test ii) we have the requirement of connected graphs, it is important to find the percolation point for random bipartite graphs. We keep the notation of the main text, and define $|P| \geq |A|$. Saltykov [32] showed that in bipartite graphs the number of isolated nodes (i.e., those that are not part of the giant component) is Poisson distributed. Using this result, Blasiak

& Durrett [33] provided the following extension: for a random bipartite graph with $|P|$ rows, $|A|$ columns and $|E|$ edges, whenever $|E| > |P| \log(|P| + |A|)$, then the graph is almost surely connected (again, for the limit $n \to \infty$).

From this, one can see that the probability of finding a connected graph approaches one whenever the probability of connection $C > |P| \log(|P| + |A|)/(|P| \cdot |A|) = \log(|P| + |A|)/|A|$.

For networks close to this threshold, it would be better to build a sampling algorithm based on Monte Carlo Markov Chain methods. For example: at each step of the algorithm, two matrix coefficients are swapped at random; if this leads to a disconnected network then the move is rejected, otherwise it is accepted. However, the mixing time of such an algorithm is unknown (the point at which the matrix can be considered sufficiently randomised).

5.3 Quantitative networks

To assess the nestedness of a quantitative incidence matrix $\mathcal{B}$ we can apply the three tests used in the binary case, but now the non-zero entries to be shuffled can take positive values other than one. We also introduce a fourth null model particular to quantitative matrices: iv) preserve $|P|$, $|A|$ and $|E|$, and shuffle the coefficient values of $\mathcal{B}$ but not their positions. That is, maintain the binary structure of the matrix (where the non-zero entries are located) but randomise which coefficient values occupy which non-zero positions. As before, the p-value is the probability that a randomly constructed matrix $\mathcal{B}'$ has spectral radius $\rho(\mathcal{A}') \geq \rho(\mathcal{A})$, where $\mathcal{A}$ and $\mathcal{A}'$ are the adjacency matrices of $\mathcal{B}$ and $\mathcal{B}'$, respectively. For test iv), the p-value is to equal one when all the coefficients have the same value (e.g., a binary matrix).

5.4 Generating random matrices

For tests i) and ii), randomised versions of the original matrix are generated using the `gsl_ran_shuffle` function included as part of the GNU Scientific Library (GSL); and for test ii) only connected graphs are retained. We checked for connectedness using a Depth First Search (DFS) algorithm

that runs in linear time. Test iii) generates randomised matrices using the "Trial swap" algorithm described in [79], which shuffles coefficient values while maintaining the original degree distribution. This algorithm has the advantage of sampling potential matrices uniformly. Test iv) uses the `gsl_ran_shuffle` function to randomise the coefficient values but not binary position of the original matrix, as required.

6 Effective abundance of quantitative bipartite networks

6.1 Empirical data

We analysed 52 bipartite ecological networks from the literature (Supplementary Table S1). The networks spanned a range of mutualistic, antagonistic and facilitative systems, and all included quantitative interaction data. We chose networks that had at least 20 species in the largest connected component and had sufficient binary links (edges) to perform nestedness test ii), i.e., connected structures could be found during network randomisation. As described in the main text (and in more detail below), we obtained quantitative preference networks from the original data, and ran nestedness tests on binary versions of the networks as well as the preference matrices. We are particularly interested in the results of test ii) for determining the nestedness of binary network structure, and quantitative test iv) for determining the nestedness of species preferences (wherein we hold the binary structure constant). Network properties and results for all seven nestedness tests are given in Supplementary Table S1.

6.2 Effective abundance, pseudo-inverse and mass action

Here we present theory underlying the normalisation of empirical quantitative data according to mass action. Data are in the form of an incidence matrix $\mathcal{B}$ with entries that record, for example, the number of visits between a pollinator species and a plant species. In the main text we suggested that the elements of $\mathcal{B}$ can be decomposed into a preference term and a mass action term (the product of interacting species effective abundances), i.e., $\mathcal{B}_{i,j} = \gamma_{i,j} x_i x_j$. Using the method outlined below

we show how effective abundances, $\hat{x}_i$ and $\hat{x}_j$ (estimated quantities will be distinguished by the "hat" symbol), can be inferred from empirical data. This allows us to rescale the incidence matrix according to mass action, leading to an estimate for species preferences: $\hat{\gamma}_{i,j} = \mathcal{B}_{i,j}/(\hat{x}_i\hat{x}_j)$. If the system follows the principle of mass action completely then the $\hat{\gamma}$-matrix is binary, and otherwise, the $\hat{\gamma}$-matrix can be tested for quantitative nestedness.

To begin, if no interaction is recorded $\mathcal{B}_{i,j} = 0$ and we set the estimate for species preference $\hat{\gamma}_{i,j} = 0$. For the remaining set of recorded counts with $\mathcal{B}_{i,j} > 0$, we take logarithms: $\log \mathcal{B}_{i,j} = \log \gamma_{i,j} + \log x_i + \log x_j$, and so under the mass action hypothesis $\log \gamma_{i,j} = 0$ which implies $\gamma_{i,j} = 1$, as required. Let us recast the log-expression as $Y_{i,j} = \alpha_{i,j}X_i + \beta_{i,j}X_j + \epsilon_{i,j}$, where $\alpha_{i,j}$ and $\beta_{i,j}$ can be thought of as regression coefficients, X_i and X_j are unknown variables, and $\epsilon_{i,j}$ is an error term. We look to minimise errors ϵ so that we may obtain best-fit effective abundances $\hat{x}_i \approx X_i$ and $\hat{x}_j \approx X_j$ for the mass action normalisation. If there are no errors—which is highly unlikely—then the estimated $\hat{\gamma}$-matrix is binary, as required; deviations from the best-fit solution give rise to $\hat{\gamma}_{i,j}$'s > 1 and $\hat{\gamma}_{i,j}$'s < 1, accordingly. In this way, the minimisation attempts to constrain the $\hat{\gamma}_{i,j}$'s to be as close to 1 as possible, and is therefore conservative in assessing quantitative preferences relative to mass action.

For illustrative simplicity, the expression $Y_{i,j} = \alpha_{i,j}X_i + \beta_{i,j}X_j + \epsilon_{i,j}$ can be written as a matrix equation of the form $y = Mx$, where we have also dropped the error term but it is still implied. The vector y contains the logarithm of empirical pairwise interaction data, M is a binary matrix indicating which species (column) are involved (entry-1) in each interaction (row), and x is an unknown vector of effective abundances. We solve $y = Mx$ for $x = M^*y$ by finding the pseudo-inverse matrix M^*. Suppose M is a $n \times m$ matrix, y is a known n-vector and x is an unknown m-vector. If $n > m$ (which is always the case for our empirical networks) then there are more constraints than unknowns, and the system is overdetermined, with no solutions (except for degenerate cases). Under this condition we can find a least-squares solution that minimises the error $(y - Mx)$.

We want to find x that minimises $||y - Mx||^2$, which can be also be written $(y - Mx)^T(y - Mx)$. This expression can be expanded: $y^Ty - y^TMx - x^TM^Ty + x^TM^TMx$. Differentiating w.r.t. x and setting the result equal to zero yields $-(y^TM)^T - (M^Ty) + 2M^TMx = 0$, and so $x = (M^TM)^{-1}M^Ty$, where $(M^TM)^{-1}M^T$ is an $m \times n$ matrix called the pseudo-inverse. We calculate the pseudo-inverse using the `pseudoinverse` function included as part of the `corpcor` package in R.

The vector x above represents entire set of effective abundances and, as stated at the beginning of this section (where the effective abundances were written $\hat{x_i}$ and $\hat{x_j}$), they can be used to obtain an estimated best-fit quantitative preference matrix: $\hat{\gamma}_{i,j} = \mathcal{B}_{i,j}/(\hat{x}_i\hat{x}_j)$.

7 Dynamical models and built-in stability

Thébault and Fontaine [9] study a system of differential equations describing obligate mutualism. (Obligate is understood to mean that species cannot survive in isolation, and therefore interaction with other species in the system is a necessary condition for existence.) They claim that "A highly connected and nested architecture promotes community stability [which they choose to define as persistence] in mutualistic networks." However, we have shown nestedness to minimise local stability. We argue that they have inadvertently built-in dynamical stability into their model, and that the positive relationship they found between nestedness in persistence actually reflects a positive relationship between connectance and persistence in obligate mutualistic systems (an argument also put forward by James *et al.* [28]). When repeating their analysis, we find nestedness to have no effect on either (dynamical) stability or persistence.

Without loss of generality, the system can be written as

$$\frac{dX_i}{dt} = X_i\left(-r_i - s_iX_i + \sum_{j\leftrightarrow i}\frac{\alpha_{ij}X_j}{h_{ij} + \sum_{k\leftrightarrow i}X_k}\right), \tag{S3}$$

where the sums are taken across all species j that are mutualists of i (denoted by $j \leftrightarrow i$) and

all parameters are positive. This system has one feasible equilibrium (besides the trivial case $X_i^* = 0 \,\forall\, i$, i.e., no species are present):

$$X_i^* = \frac{\left(-r_i + \sum_{j \leftrightarrow i} \frac{\alpha_{ij} X_j}{h_{ij} + \sum_{k \leftrightarrow i} X_k}\right)}{s_i}. \tag{S4}$$

Simulations demonstrate that the diagonal elements of the community matrix M (the Jacobian matrix evaluated at equilibrium), $M_{ii} = -s_i X_i^*$, dominate the corresponding row—a phenomenon known as diagonal dominance. That is, $|M_{ii}| > \sum_j |M_{ij}|$, for all i, which is a sufficient condition for dynamical stability (see main text). Hence, all feasible equilibria ($X_i^* > 0 \,\forall\, i$) are necessarily stable *irrespective* of nestedness (or, in fact, any other configuration of interactions).

It has been shown for systems very similar to those examined here that local stability implies global stability [80]. This indicates that all orbits in the positive orthant of phase space are attracted to the equilibrium point, and such systems are guaranteed to be stable irrespective of initial conditions. The one difference in the model Thébault & Fontaine consider is that a negative intrinsic rate of species increase, $-r_i$, is used rather than a positive rate r_i.

Using this slightly different model, Thébault & Fontaine describe a positive effect of nestedness on the probability of reaching a feasible equilibrium (persistence). With a negative intrinsic rate of increase $-r_i$, species with densities close to zero will go extinct unless they have sufficient mutualistic partners to "pull" the species to larger density. A disconnected species would necessarily go extinct (due to obligate mutualism), and a species with few interaction partners would be more likely to go extinct than one that is well connected. Because of this fact, connectance—and not nestedness—should be important for persistence.

We repeated the experiments of Thébault & Fontaine for different levels of connectance and measured the correlation between nestedness and persistence for a given connectance. The results show that nestedness produces no significant trend, whereas connectance is essential for persistence, in line with our argument (Supplementary Figure S7).

Supplementary References

[34] De Sassi, C. Data. *unpublished* (2XXX).

[35] Tylianakis, J.M., Tscharntke, T. & Klein, A.-M. Diversity, ecosystem function, and stability of parasitoid–host interactions across a tropical habitat gradient. *Ecology* **87**, 3047–3057 (2006).

[36] Verdú, M. & Valiente-Banuet, A. The relative contribution of abundance and phylogeny to the structure of plant facilitation networks. *Oikos* **120**, 1351–1356 (2011).

[37] Arthur, J.R., Margolis, L. & Arai, H.P. Parasites of fishes of aishihik and stevens lakes, yukon territory, and potential consequences of their interlake transfer through a proposed water diversion for hydroelectrical purposes. *Journal of the Fisheries Research Board of Canada* **33**, 2489–2499 (1976).

[38] Leong, T.S. & Holmes, J.C. Communities of metazoan parasites in open water fishes of cold lake, alberta. *Journal of Fish Biology* **18**, 693–713 (1981).

[39] Dechtiar, A.O. Parasites of fish from lake of the woods, ontario. *Journal of the Fisheries Research Board of Canada* **29**, 275–283 (1972).

[40] Arai, H.P. & Mudry, D.R. Protozoan and metazoan parasites of fishes from the headwaters of the parsnip and mcgregor rivers, british columbia: a study of possible parasite transfaunations. *Canadian Journal of Fisheries and Aquatic Sciences* **40**, 1676–1684 (1983).

[41] Bangham, R.V. Studies on fish parasites of lake huron and manitoulin island. *American Midland Naturalist* **53**, 184–194 (1955).

[42] Chinniah, V.C. & Threlfall, W. Metazoan parasites of sh from the smallwood reservoir, labrador, canada. *Journal of Fish Biology* **13**, 203–213 (1978).

[43] Blüthgen, N. & Fielder, K. Competition for composition: Lessons from nectar-feeding ant communities. *Ecology* **85**, 1479–1485 (2004).

[44] Fonseca, C.R. & Ganade, G. Asymmetries, compartments and null interactions in an amazonian ant-plant community. *Journal of Animal Ecology* **66**, 339–347 (1996).

[45] Bezerra, E.L.S., Machado, I.C. & Mello, M.A.R. Pollination networks of oil-flowers: a tiny world within the smallest of all worlds. *Journal of Animal Ecology* **78**, 1096–1101 (2009).

[46] Kaiser-Bunbury, C.N., Memmott, J. & Müller, C.B. Community structure of pollination webs of mauritian heathland habitats. *Perspectives in Plant Ecology, Evolution and Systematics* **11**, 241–254 (2009).

[47] Kevan, P.G. *High arctic insect-flower visitor relations*. Ph.D. thesis, University of Alberta (1970).

[48] Inouye, D.W. & Pyke, G.H. Pollination biology in the snowy mountains of australia: comparisons with montane colorado, usa. *Australian Journal of Ecology* **13**, 191–210 (1988).

[49] Memmott, J. The structure of a plant-pollinator food web. *Ecology Letters* **2**, 276–280 (1999).

[50] Mosquin, T. & Martin, J.E.H. Observations on the pollination biology of plants on melville island, n.w.t., canada. *Canadian Field Naturalist* **81**, 201–205 (1967).

[51] Motten, A.F. Pollination ecology of the spring wildflower community of a temperate deciduous forest. *Ecological Monographs* **56**, 21–42 (1986).

[52] Olesen, J.M., Eskildsen, L.I. & Venkatasamy, S. Invasion of pollination networks on oceanic islands: importance of invader complexes and endemic super generalists. *Diversity and Distributions* **8**, 181–192 (2002).

[53] Ollerton, J., Johnson, S.D., Cranmer, L. & Kellie, S. The pollination ecology of an assemblage of grassland asclepiads in south africa. *Annals of Botany* **92**, 807–834 (2003).

[54] Schemske, D.W. *et al.* Flowering ecology of some spring woodland herbs. *Ecology* **59** (1978).

[55] Small, E. Insect pollinators of the mer bleue peat bog of ottawa. *Canadian Field Naturalist* **90**, 22–28 (1976).

[56] Vázquez, D.P. & Simberloff, D. Ecological specialization and susceptibility to disturbance: conjectures and refutations. *American Naturalist* **159**, 606–623 (2002).

[57] Lafferty, K.D., Dobson, A.P. & Kuris, A.M. Parasites dominate food web links. *Proceedings of the National Academy of Sciences* **103**, 11211–11216 (2006).

[58] Beehler, B. Frugivory and polygamy in birds of paradise. *The Auk* **100**, 1–12 (1983).

[59] Poulin, B., Wright, S.J., Lefebvre, G. & Calderon, O. Interspecific synchrony and asynchrony in the fruiting phenologies of congeneric bird-dispersed plants in panama. *Journal of Tropical Ecology* **15**, 213–227 (1999).

[60] Schleuning, M. *et al.* Specialization and interaction strength in a tropical plant–frugivore network differ among forest strata. *Ecology* **92**, 26–36 (2010).

[61] Snow, B.K. & Snow, D.W. The feeding ecology of tanagers and honeycreeperes in trinidad. *The Auk* **88**, 291–322 (1971).

[62] Snow, B.K. & Snow, D.W. *Birds and Berries* (Calton, England, 1988).

[63] Sorensen, A.E. Interactions between birds and fruit in a temperate woodland. *Oecologia* **50**, 242–249 (1981).

[64] Baird, J.W. The selection and use of fruit by birds in an eastern forest. *The Wilson Bulletin* **92**, 63–73 (1980).

[65] Carlo, T.A., Collazo, J.A. & Groom, M.J. Avian fruit preferences across a puerto rican forested landscape: Pattern consistency and implications for seed removal. *Oecologia* **134**, 119–131 (2003).

[66] Dicks, L.V., Corbet, S.A. & Pywell, R.F. Compartmentalization in plant-insect flower visitor webs. *Journal of Animal Ecology* **71**, 32–43 (2002).

[67] Frost, P. Fruit-frugivore interactions in a south african coastal dune forest. In *Fruit-frugivore interactions in a South African coastal dune forest*, 1179–1184 (Acta 17th Congr. Intern. Ornithol., 1980).

[68] Galetti, M. & Pizo, M.A. Fruit eating birds in a forest fragment in southeastern brazil. *Ararajuba* **4**, 71–79 (1996).

[69] Jordano, P. El ciclo anual de los paseriformes frugívoros en el matorral mediterráneo del sur de españa: importancia de su invernada y variaciones interanuales. *Ardeola* **32**, 69–94 (1985).

[70] Jordano, P. Data. *unpublished* (2XXX).

[71] Chacoff, N.P. *et al.* Evaluating sampling completeness in a desert plant-pollinator network. *Journal of Animal Ecology* **81**, 190–200 (2012).

[72] Noma, N. Annual fluctuations of sapfruits production and synchronization within and inter species in a warm temperature forest on yakushima island. *Tropics* **6**, 441–449 (1997).

[73] Yodzis, P. & Winemiller, K.O. In search of operational trophospecies in a tropical aquatic food web. *Oikos* **87**, 327–340 (1999).

[74] Désesquelles, P. Calculation of the number of partitions with constraints on the fragment size. *Physical Review C* **65**, 34603–34603 (2002).

[75] Ruskey, F. Combinatorial generation. *Working Version (1j-CSC 425/520)* (2003).

[76] Stewart, W.J. *Introduction to the Numerical Solution of Markov Chains* (Princeton University Press, 1994).

[77] Bryan, K. & Leise, T. The $25,000,000,000 Eigenvector: The Linear Algebra behind Google. *SIAM Review* **48**, 569–582 (2006).

[78] Canfield, E.R., Greenhill, C. & McKay, B.D. Asymptotic enumeration of dense 0–1 matrices with specified line sums. *J. Comb. Theory Ser. A* **115**, 32–66 (2008).

[79] Miklós, I. & Podani, J. Randomization of presence–absence matrices: Comments and new algorithms. *Ecology* **85**, 86–92 (2004).

[80] Smith, H.L. On the asymptotic behavior of a class of deterministic models of cooperating species. *SIAM Journal on Applied Mathematics* **46**, 368–375 (1986).